

Journal of Optimization in Soft Computing (JOSC)

Vol. 2, Issue 4, pp: (56-65), Winter-2024 Journal homepage: https://sanad.iau.ir/journal/josc

Paper Type (Research paper)

Optimal use of photovoltaic systems in the distribution network considering the variable load and production profile of Kerman city

Fahimeh Sayadi Shahraki¹, Shaghayegh Bakhtiari Chehelcheshmeh^{2*} and Alireza Zamani nouri³

- 1. Department of Electrical Engineering, Shahr-e-Qods Branch, Islamic Azad University, Tehran, Iran.
- 2. Department of Computer Engineering, Shahrekord Branch, Islamic Azad University, Shahrekord, Iran.
 - 3. Department of Civil Engineering, Shahr-e-Qods Branch, Islamic Azad University, Tehran, Iran.

Article Info

Article History:

Received: 2025/01/01 Revised: 2025/03/15 Accepted: 2025/04/05

DOI:

Keywords:

Photovoltaic systems,

Optimization, distribution network, power quality

*Corresponding Author's Email Address: sh.bakhtiari@iaushk.ac.ir

Abstract

Photovoltaic systems are very important renewable energy sources, and optimal use of their active and reactive power capacity is very useful in improving the power quality of the distribution network. Therefore, it is necessary to determine the optimal location, number, and capacity of the solar system with appropriate optimization methods so that the maximum reduction in network losses is achieved while considering power quality constraints. Given the complexity and many limitations of the problem, the need to use an appropriate optimization method is evident. In this paper, using the P-PSO optimization algorithm, in the IEEE 33-bus test network, the location and capacity of the active and reactive power of the solar system are determined based on the variable load profile of the network and the daily production curve of the solar system in Kerman city to minimize losses and improve the voltage profile of the electrical energy distribution networks. To increase the accuracy of this optimization, each of the load and production curves is divided into three different levels, according to the geographical climate of Kerman city, in one year, and to evaluate the performance of the proposed method, the relevant results in four different scenarios are examined. The optimization results indicate a significant impact on improving power quality indicators in the presence of photovoltaic systems, especially when using the active and reactive power capacities of these units simultaneously.

1. Introduction

Increasing air pollution and shortage of fuel for fossil power plants in the world have led to an increasing interest in clean and renewable sources. On the other hand, the electrical energy distribution network has faced an increasing load demand, which highlights the need to use local production sources. Solar or photovoltaic systems are among the renewable distributed generation sources that include various advantages such as environmental compatibility, flexibility, reliability, and economic benefits [1]. So far, many studies have been conducted on the connection of distributed generation to the distribution network, and many

countries are turning to these sources due to the environmental, economic, and reliability benefits of these systems [2]. Research shows that the way of use, type, capacity, and installation location of these sources are very important in their efficiency in improving the conditions of the distribution system and power quality parameters [3]. Failure to use properly and improper determination of the capacity and installation location of these sources can even lead to a decrease in power quality in the distribution network [4]. In [5-8], the location of distributed generation in the distribution network has been carried out based on various optimization

algorithms to reduce losses. The objective function in [5-6] is to reduce losses and costs of distributed generation units. In reference [6], in addition to power losses and installation costs of distributed generation sources, the cost of air pollution is also included in the objective function. In [7-8], power quality constraints have also been evaluated in the process of installing and operating new and renewable energy sources, and the optimal location of distributed generation sources has been carried out by an optimization problem. Although the load and generation profiles of all distributed generation sources in both studies are considered constant in the distribution network. In [9], the effective use of solar systems in a distribution network that is faced with an increase in demand has been investigated. The active power generation capacity has been calculated using environmental conditions, but the reactive power capacity of these sources has not been used. In [10], recommendations and guidelines for the location and capacity of solar system installation in the existing network have been provided for power companies. Given the complexity of the optimization problem in many past studies, this problem has been modeled with various optimization methods, and researchers have tried to optimize their response using newer and more effective optimization methods and considering more constraints [11-13]. In [11], the optimization of the location of distributed generation units is proposed using improved optimization techniques, and finally, the efficiency of the proposed method compared to traditional methods has been shown.

In [12], the optimal placement of distributed generation was carried out by considering high harmonic loads in the network, and the harmonic distortion index was also stated as one of the constraints of the problem. The goal of optimization is to improve the power quality indicators in the system, and only the active power capacity of photovoltaic systems was used. In [14], the capacity and location of solar distributed generation were optimized. To limit the search space, the sensitive buses of the system were initially determined through sensitivity analysis. The load change profile and the production rate of the solar system were not considered in the presented model. In the reviewed studies, the load profile of the network and the production of distributed sources were not considered, but in some studies such as [15], the information on the consumed load in 24 hours and the average active power produced by the solar system were used to determine the optimal location and capacity of the solar system to reduce losses and reduce voltage deviation.

A review of previous studies reveals the following weaknesses:

- 1- In studies of the use of distributed generation sources from the point of view of the power quality of the distribution network, the use of the average load profile and the average production power of hypothetical distributed generation systems is completely unattainable, and naturally, due to the variability of the load profile and production, the use of the results in practice will not be very effective.
- 2- In some distributed generation sources, including photovoltaic systems, it is possible to use reactive power capacity if accurately modeled and the available range is determined, which has often been ignored in previous studies.

In the present study, to determine the installation location and the required active and reactive power utilization capacity of photovoltaic sources, the change in the actual annual load profile in Kerman been considered along with accurate information on the active power production rate of the existing solar system in Kerman. The leveling method takes into account different levels of annual load and production, and as a result of the intersection of these levels, all different load and production level states are extracted, optimization is carried out based on all levels to reduce losses and network voltage deviation. The answer to the optimization problem is the active and reactive power capacity and the location of the solar system at each load level. Also, the grid voltage constraints, the active and reactive power capacity of the photovoltaic system, and the total power generated based on demand are also considered in solving the optimization problem.

The rest of the paper is organized as follows. In section 2 solution method consist of objective function and constraints formulations are presented. Section 3 Describes how to implement the proposed method of intersecting load and production levels and P-PSO method. Simulation scenarios and results are provided in section IV and section V discusses the results and concludes the paper.

2. Solution method

2.1. Objective function

The goal of optimization is to reduce active losses and maintain the bus voltage profile within the desired range. The objective function F is defined as equation (1) which must be minimized. The weighting coefficients k_1 and k_2 are chosen between 0 and 1 and their sum is equal to one and

shows the degree of influence of each objective function on the overall objective function.

$$F = k_1 f_1 + k_2 f_2 \tag{1}$$

The first objective function f_1 is the total real losses in the buses, which is obtained from equation (2). The second objective function f_2 is the improvement rate of the voltage profile, which is defined as the sum of the squares of the bus voltage difference to the nominal value of one per unit, and is obtained from equation (3).

$$f_1 = \sum_{i=1}^{N_{bus}} \frac{Ploss_i \ with \ out \ DG}{Ploss_i \ with \ DG}$$
 (2)

$$f_2 = \sum_{i=1}^{N_{bus}} (v_i - v_{nom})^2$$
 (3)

Ploss is the total bus losses and N_{bus} is the number of busses

In order to normalize the objective function of the problem, in equation (2), the total bus losses without installing distributed generation sources are divided by the total losses in the presence of distributed generation sources. v_i is the voltage of the ith bus, v_{nom} is the nominal voltage in terms of per unit.

2.2. Constraints

2.2.1. Power balance constraint

According to equation 4, where P_{Di} , P_{PVi} are the active power generated by DG and the active power consumed in the nth bus, respectively, and P_L represents the active losses in the network in question. P_{slack} is the transmitted power from the upstream network.

$$\sum_{i=1}^{N} P_{PVi} + P_{slack} = \sum_{i=1}^{N} P_{Di} + P_{L}$$
 (4)

2.2.2. Active and reactive power generation range by solar DG

The active generation power limit of the jth distributed generation unit is obtained from equation (5).

$$P_{jPVmin} < P_j < P_{jPVmax} \quad j = 1.2....N_{DG}$$
 (5)

 N_{DG} is the number of distributed generation, P_{PVmin} is the minimum active power generated, P_{PVmax} is the maximum active power generated. In this paper, the following method is used to obtain the reactive power range:

At any time of the day, the reactive power generated by the photovoltaic system is limited by

various constraints depending on the operating point of the system, and the reactive power exchanged between the grid and the photovoltaic system converter. We assume that the PV system with the maximum active power is in the system. One of the most important constraints for the reactive power of the system is determined by the maximum apparent power of the inverter. The reactive power of the PV depends on the maximum voltage and current values of its converter, so to calculate the controllable limit Q_{PV} - P_{PV} , the maximum voltage and current values of the converter V_{Crmax} and I_{Crmax} must be considered. The relationship between active and reactive power considering the converter current is as follows:

$$P_{PV}^2 + Q_{PV}^2 = (I_C V_{PV})^2 (6)$$

And the relationship between active and reactive power, taking into account the voltage limitation of the converter, is as follows:

$$P_{PV}^2 + (Q_{PV} + \frac{V_{PV}^2}{X_C})^2 = (\frac{V_C V_{PV}}{X_C})^2$$
 (7)

Using this relationship, the design value V_{Crmax} can be calculated, which determines the maximum inverter dc link voltage V_{dcmax} and I_{Crmax} [17-18]. The maximum converter current should be in the following relationship using the values of PV voltage, active and reactive power:

$$I_{C'max} = \frac{P_{PV'R}^2 + (V_{PV'R} \tan \theta_R)}{V_{PV'min}}$$
 (8)

The maximum converter voltage is also calculated from the active and reactive power values and the maximum PV voltage as follows:

$$V_{C'max} = \frac{X_C}{V_{PV'max}} \sqrt{P_{PV'R}^2 + (V_{PV'} tan\theta_R + \frac{V_{PV'max}^2}{X_C})^2}$$
(9)

Also, the PV reactive power, taking into account the rated current and rated voltage of the PV system, is:

$$Q_{c'PV}^{t} = \sqrt{(V_{PV}I_{C'max})^2 - P_{PV}^{t^2}}$$

$$Q_{v'V}^{t} = \sqrt{(\frac{V_{C'max}V_{PV}}{X_C})^2 - P_{PV}^{t^2} - \frac{V_{PV}^2}{X_C}}$$
(10)

Finally, at each operating point, the maximum reactive power at each hour t is obtained using the following equation:

$$Q_{PV'max}^t = min\{Q_{c'PV}^t Q_{v'PV}^t\}$$
 (11)

In this article, V_{PVrmax} =1.05, V_{PVrmin} =0.95, and X_C =0.3 are considered.

3.2.3. Bus voltage limit

In equation (12), the minimum and maximum allowable voltage limits for all buses are considered to be 0.9 to 1.01 per unit. Where V_i is the voltage of the i-th bus, $V_{i.min}$, $V_{i.max}$ are the minimum and the maximum bus voltage respectively.

$$V_{i.min} < V_i < V_{i.max} \quad i = 1.2....N_{bus}$$
 (12)

3. Proposed intersection of load and production levels method and solving by P-PSO

To bring the results of the optimization problem closer to reality, changes in the load curve and solar system production should be included in the problem. In this paper, for more realistic results and to increase the optimization accuracy, changes in the load and production curve are considered in a one-year period. Since temperature changes in the seasons are the most important parameter affecting the load in the short term, the annual load curve of the Kerman city network is divided into three conditions: maximum, minimum, and intermediate temperatures, and as a result, load consumption. Kerman's peak load occurs in the summer season and the high load level occurs in this time period. In winter, due to the city's temperate geographical location and the major use of gas in heating devices, the amount of electricity used is low and the low load level occurs in this period. Finally, in the temperate seasons of autumn and spring, load consumption is considered as the medium load level. Accordingly, the load curve of Kerman city is divided into three low load, high load, and medium load levels in a year based on seasonal changes, as shown in Table 1. Also in Table 2, the active and reactive power capacity of the photovoltaic system is specified for each load level.

Table 1. Network load levels studied in one year

Load Levels	month of the year
Low load	November, December, January, February
Mid load	April, May, October, March
High load	June, July, August, September

Table 2. Active and reactive power of the photovoltaic system for each load level

system for each four level								
	Active power	Reactive power						
Test network	P	Q						
Low load	0.3P	1.5Q						
Mid load	0.6P	0.5Q						
High load	P	Q						

Table 3. Yearly leveling the solar system production curve

Load Level	months	Capacity factor percentage	Probability of occurrence per
Low load	August, November,	74%	year 4
Low load	-	7470	<u> </u>
	December, January		12
Mid load	April, May, February,	90%	4
	March		$\overline{12}$
High load	June, July, September,	100%	4
_	October		12

Solar cells rarely operate at their maximum power point because the output power is affected by radiation and ambient temperature. Load changes also affect the shift of the operating point and the power received from the system. By studying the energy output of the solar system in the geographical area of Kerman, the production curve of the photovoltaic system is obtained at three different levels low load, medium load, and high load according to Table 3.

3.1. Intersection of the load and production curves

In this paper, to increase the accuracy of the obtained results, it is used to consider different states of the curve resulting from the intersection of two load curves and the solar system production curve. Since three levels (low load, medium load, and high load) are considered for the load and production curve, the resulting curve has 9 states, but with the assumptions of the problem for the city of Kerman, only 6 of these 9 states occur. The intersection of the two curves is shown in Figure 1.

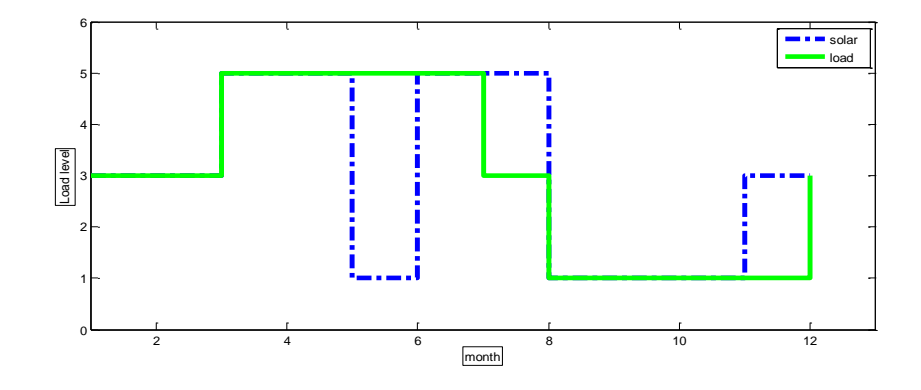


Figure 1. The intersection of two annual load and production graphs of a solar system

The characteristics of the different states of the graph resulting from the intersection of the two load and production curves are presented in Table 4. Accordingly, in order to solve the problem in question, by determining the loss objective function for each of these 6 states, according to equation (13), the objective function of the problem is obtained by considering the changes in the load curve and the changes in the production curve.

$$F_T = \frac{3}{12}g1 + \frac{3}{12}g2 + \frac{3}{12}g3 + \frac{1}{12}g4 + \frac{1}{12}g5 + \frac{1}{12}g6$$
 (13)

First case: For the months of November-December-January, the load curve and the generation curve are at low load level. Therefore, the coefficient of the corresponding loss function

g1 is obtained as 3/12. The generation capacity factor is 74%. (For load distribution) its active power is considered to be 0.3 times the active power of the test network load and its reactive power is considered to be 1.5 times the reactive power of the test network.

Second case: In the months of June, July, and September, the load curve and the generation curve are at medium load level, therefore the coefficient of the corresponding loss function g2 is obtained as 3/12. The generation capacity factor is 90%. (For load distribution) its active power is considered to be 0.6 times the active power of the test network load and its reactive power is considered to be 0.5 times the reactive power of the test network. The table below describes the status of all 6 possible cases.

Mid	Mid	High	High	Low	Low	Mid	High	Low	Load Level
High	Low	Mid	Low	Mid	High	Mid	High	Low	Generation Level
1 12	0	0	$\frac{1}{12}$	1 12	0	3 12	3 12	3 12	Probability
October	Don't occure	Don't occure	August	February	Don't occure	April May March	June July September	November December January	Month
0.6P	0.6P	Р	P	0.3P	0.3P	00.6P	Р	0.3P	Active power
0.5Q	0.5Q	Q	Q	1.5Q	1.5Q	0.5Q	Q	1.5Q	Reactive power
100%	74%	90%	74%	90%	100%	90%	100%	74%	Capacity factor

Table 4. All possible load and production states and 6 possible states

3.2. Problem-solving with the P-PSO algorithm

To solve the optimization problem described in this section, a new and very effective and useful algorithm, P-PSO, has been used, the capabilities and implementation of which are shown in [17].

Despite the competitive performance of PSO, it is noted the tendency of PSO swarm to converge prematurely in the local optima, due to its rapid convergence on the best position found so far at the early stage of optimization. Main challenging issue that needs to be addressed is the proper control on the exploration and exploitation searching of PSO. *Basic PSO Algorithm*

In basic PSO, each particle that is roaming through the D dimensional problem hyperspace represents the potential solution for a specific problem. For particle i two vectors, i.e. position vector $X_i =$ $[X_{i1}, X_{i2}, ..., X_{iD}]$ and velocity vector $V_i =$ [V_{i1} ·V_{i2} · ... · V_{iD}] are used to represent its current state. Additionally, each particle i can memorize its personal best experience ever encountered (i.e. cognitive experience), represented by the personal best position vector $P_i = [P_{i1}, P_{i2}, ..., P_{iD}]$. The position attained by the best particle in the society (i.e. social experience) is represented $asP_g =$ $[P_{g1}, P_{g2}, ..., P_{gD}]$. Mathematically, at iteration (t + 1) of the searching process, the d-th dimension of particle i's velocity, $V_{id}(t + 1)$ and position $X_{i,d}(t + 1)$ are updated as follows:

$$V_{id}(t+1) = V_{id}(t) + c_1 r_1 (P_{id}(t) - X_{id}(t)) + c_2 r_2 (P_{gd}(t) - X_{id}(t))$$

$$X_{id}(t+1) = X_{id}(t) + V_{id}(t+1)$$
(14)
(15)

Where c_1 and c_2 are the acceleration coefficients; r_1 and r_2 are two random numbers generated from a uniform distribution within the range of [0, 1]. Particles velocity is clamped to a maximum magnitude of V_{max} to prevent swarm explosion. When minimizing the fitness function f in D dimensional search space, particle i's P_i position in iteration (t+1) is updated as follows [19]:

$$P_i(t+1) = \begin{cases} X_i(t+1) & if \ f(X_i(t+1)) < f(P_i(t)) \\ P_i(t) & other \ wise \end{cases}$$
(16)

P-PSO Algorithm

Despite the competitive performance of PSO, researchers have noted the tendency of PSO swarm to converge prematurely in the local optima, due to its rapid convergence on the best position found so far at the early stage of optimization [20]. Once the swarm congregates at such position, little opportunity is afforded for the population to explore for other solution possibilities by designing perturbation module. This leads to the entrapment of the swarm within the local optima of search space and thus premature convergence occurs. Another challenging issue that needs to be addressed is the proper control on the exploration

$$\begin{aligned} P_{gd}^{per} &= \\ \left\{ P_{gd} + r_4 \big(X_{max,d} - X_{min,d} \big) & \text{if } r_3 > 0.5 \\ P_{gd} - r_4 \big(X_{max,d} - X_{min,d} \big) & \text{if } r_3 \leq 0.5 \end{aligned} \right. \end{aligned}$$

and exploitation searching of the PSO. So P- PSO which was proposed in [17] is characterized by:

3.2.1 Velocity calculation

In this model to achieve better control on the algorithm's exploration and exploitation capabilities, particles velocity is dependent on both particle's fitness and time. More specifically, particles with better (i.e. lower) fitness value are assigned with lower ω_i that favour the exploitation, whilst particles with worse (i.e. higher) fitness value is encouraged for the exploration by assigning them with higher ω_i . Mathematically, particle i's inertia weight, i.e. ω_i is calculated as follows:

$$\omega_{i} = c_{1} \left((\omega_{max} - \omega_{min}) * G_{i} + \omega_{min} \right) + c_{2} \left((\omega_{max} - \omega_{min}) * \frac{maxiter - iter}{maxiter} + \omega_{min} \right)$$
(17)

Where ω_{max} and ω_{min} represent the maximum and minimum inertia weights, respectively, i.e. $\omega_{max} = 0.9$ and $\omega_{min} = 0.4$; G_i represents the fitness dependent weight value that determines ω_i of particle i as shown:

$$G_i = \frac{f(P_i) - f_{min}}{f_{max} - f_{min}} \tag{18}$$

Where f_{max} and f_{min} represent the maximum and minimum personal best fitness values that exist in the population. Equation (18) shows that the particle with smaller fitness has smaller and thus is assigned with smaller ω_i and vice versa. To this end, we update the particle i's velocity, V_i as follows:

$$V_i(t+1) = \omega_i V_i + \sum_{P_k \in N_i} c_k r_k (P_k - X_i)$$
 (19) where P_k represents the personal best position of neighboring particles that exist in particle i's neighborhood; N_i represents the number of neighbouring particles available for particles); c_k represents the acceleration coefficient that equally distributed among the N_i neighboring particles, calculated as, $c_k = c/N_i$ where; $c = 4.1$, r_k represents the random number in the range of [0, 1].

3.2.2 Perturbation module

To alleviate the premature convergence issue, a perturbation module is adopted to perform perturbation on the P_g particle and provide extra diversity for it to jump out from local optima, if its fitness is not improved for m successive function evaluations (FEs). The m value that used to trigger perturbation module should not be set too large or too small, as the former wastes the computation resources, whilst the latter degrades algorithm's convergence speed. Herein, m is set as 5. In perturbation module, one of the d-dimension of P_g particle i.e. P_{gd} is first randomly selected and it is then perturbed randomly by a normal distribution as follows:

Where P_{gd} , is the perturbed P_g ; r_3 is a random number with the range of [0, 1] and generated from uniform distribution; r_4 is a random number generated from the normal distribution of $N \sim (\mu, \sigma^2)$ with mean value of $\mu = 0$ and standard deviation of $\sigma = R$, respectively. R represents the perturbation range that linearly decreased with the number of FEs as follows:

$$R = R_{max} - (R_{max} - R_{min}) \frac{fes}{FE_{max}}$$
 (21)

Where R_{max} and R_{min} are the maximum and minimum perturbation ranges, respectively; fes is the FEs number used; max FE is the predefined maximum FEs. The newly perturbed P_g particle, i.e. P_g^{per} is then evaluated and examined. It will replace P_g if $f(P_g^{per}) < f(P_g)$.

The process of solving the aforementioned optimization problem is shown in the flowchart in Figure 2.

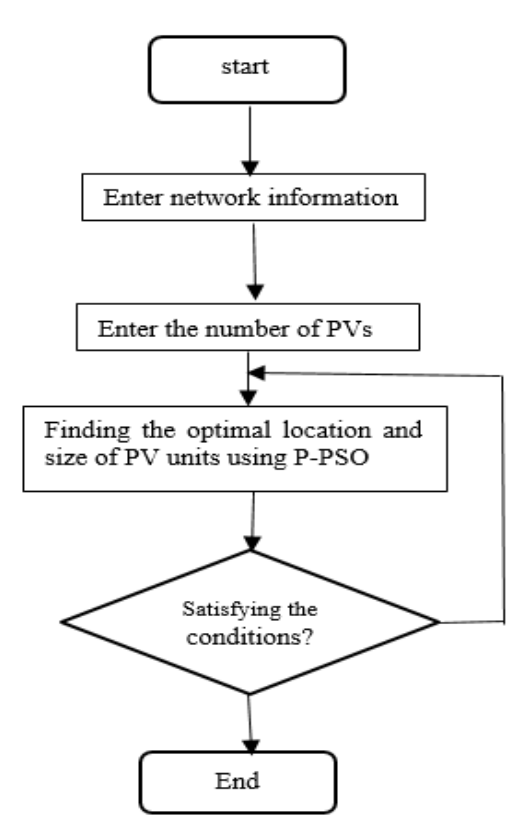


Figure 2. Problem-solving algorithm

4. Numerical results

The maximum number of distributed generation sources is four and the generation capacity range of each DG unit is 1.2 MW and 1.2 MVAR.

To show the effect of using the reactive power capacity of PV systems and also to evaluate the proposed method on the selection of optimal location and capacity, simulations(183)ve been performed considering four scenarios:

- 1- The studied network without the presence of distributed generation such as photovoltaic systems
- 2- The network in the presence of photovoltaic systems and assuming only the use of active power
- 3- The network in the presence of photovoltaic systems and assuming the production of active and reactive power
- 4- Similar to case 3 but without leveling (assuming the average load and production).

In this paper, the role of reducing losses and improving the voltage profile in the equal objective function is considered ($K^{\}=K2=0.5$).

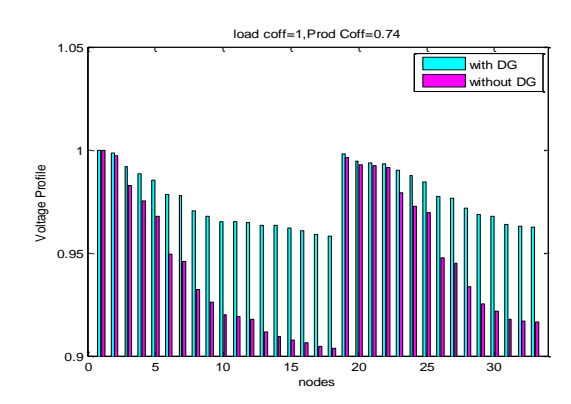


Figure 1. Intersection of two annual

Table 5.	Voltage deviation	changes	in four	scenarios

Avera		6	5	4	3	2	1	states
6 E	Load factor	0.3	0.6	1	0.3	0.6	1	Sce
	Generation factor	0.9	1	0.74	0.74	0.9	1	nario

	V.D6	V.D5	V.D4	V.D3	V.D2	V.D1	
	-	0.0599	0.0402	0.1338	0.0599	0.0402	1
0.1947	0.1579	0.0314	0.4052	0.2500	0.0652	0.2654	2
0.0541	0.0002	0.0036	0.0245	0.0021	0.0012	0.0077	3
0.0583	0.0105	0.18	0.1374	0.0114	0.0847	0.028	4

Table 6. Capacity and location of installed PV units

PV 4	PV 4		PV 3		PV 2		PV 1	
Capacity	Location	Capacity	Location	Capacity	Location	Capacity	Location	
P(kW)		P(kW)		P(kW)		P(kW)		
Q(kVAR)		Q(kVAR		Q(kVAR)		QkVAR		
-	-	-	-	-	-	-	-	1
473.40	31	444.43	14	642.82	6	661.04	24	2
0		0		0		0		
631.72	24	439.78	7	451.3	14	576.7	30	3
388.59		391.38		288.56		759.21		
741.66		588.7		535.6		953.4		
448.11	14	516.43	30	649.20	6	670.63	24	4
329.59		966.1		535.63		480.81		

Table 7. Power loss in four scenarios

		Load 0.3	0.6	1	0.3	0.6	1	
PLOSS _{MID} .	PLOSSave	Generation 0.9	1	0.74	0.74	0.9	1	Scenario
		F6	F5	F4	F3	F2	F1	
	-	159.52	63.91	210.99	159.52	63.91	210.99	1
	0.5355	0.9575	0.286	0.475	0.9186	0.2688	0.3816	2
	0.1888	0.2655	0.1987	0.2099	0.3074	0.1289	0.0941	3
0.1124	0.2136	0.1899	0.4232	0.1709	0.2188	0.2883	0.0858	4

The results of Table 5 show that the optimal use of active and reactive power capacity can be effective in reducing voltage deviation. So scenario 3 shows the lowest voltage deviation. Table 6 shows the results of the capacity and location of installed PV units. To evaluate the results from the point of view of losses, Table 7 summarizes the results of the different objective functions and also reports the average losses. As can be seen in scenario 1, losses occur at the highest level and the use of the active power capacity of the photovoltaic system leads to

a significant reduction in the level of power losses in the network. Also, comparing the results of the second and third scenarios shows the effect of using the reactive power capacity of the photovoltaic system in reducing losses. So at peak load, losses are reduced to about one-third. To see the effect of using the photovoltaic system, the voltage results of all buses at peak load in the first and third scenarios are shown in Figure 3. According to the figure, in the third scenario, due to the simultaneous use of the active and reactive power capacity of the solar system, the bus voltage deviation level is minimized. The results of Table

6 show that the use of reactive and active power capacity simultaneously with the proposed leveling method is effective in controlling the bus voltage deviation, reducing losses, and reducing system costs. To see the importance of using the proposed leveling method, the results of the third and fourth scenarios can be compared. As can be seen, the voltage deviation at peak load in the third scenario is about one-sixth of that in the fourth scenario, and the power losses in the third scenario are less than half of those in the fourth scenario.

These results reveal the importance of load and generation leveling according to climate in the use of distributed generation resources.

Figure 4 shows the convergence plot of the P-PSO method compared to PSO. Comparing the two plots reveals the optimization quality and escape from the local convergence of P-PSO.

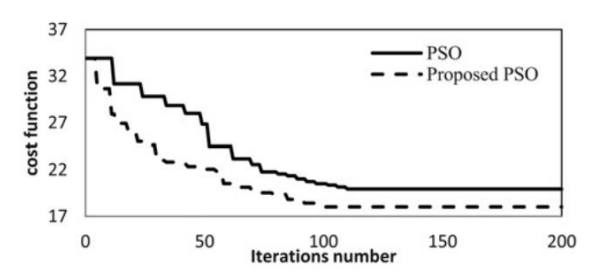


Figure 4. Convergence diagram of P-PSO and PSO methods

5. Conclusion

In this paper, the location and capacity of the active and reactive power of the photovoltaic system in the distribution network were optimized based on the load leveling required and the generation capacity of the photovoltaic system. The aim of optimizing the voltage and reactive power control in the network under study was to reduce active power losses and bus voltage deviations as the main objectives. To use the leveling method, the actual load and generation profile of Kerman was used, and the results obtained indicate the importance of proper use of distributed generation resources and the advantage of using the reactive power capacity of these systems. Observation of the results shows that the use of the photovoltaic system leads to a profound reduction in active losses and bus voltage deviations in the system. However, using the reactive power capacity of these resources compensates the system voltage level more appropriately. Of course, it is necessary to consider the limitations of the active and reactive power generated by these distributed generation resources. Also, the use of the P-PSO optimization method shows the appropriate quality of

optimization of this method and the escape from local convergence in complex problems. The results of the article show that the appropriate use of the leveling method in a distribution system with distributed generation resources will lead to improved results and achieve the goal of improving power quality in the network.

References

- [1] M. C. V. Suresh and E. J. Belwin, "Optimal DG placement for benefit maximization in distribution networks by using dragonfly algorithm," Renewables Wind Water and Solar, vol. 5, pp. 2–8, 2018.
- [2] T. D. Pham, T. T. Nguyen, and B. H. Dinh, "Find optimal capacity and location of distributed generation units in radial distribution networks by using enhanced coyote optimization algorithm," Neural Computing & Applications, vol. 33, pp. 4343–4371, 2021.
- [3] A. Rathore and N. P. Patidar, "Optimal sizing and allocation of renewable based distribution generation with gravity energy storage considering stochastic nature using particle swarm optimization in radial distribution network," Journal of Energy Storage, vol. 35, p. 102282, 2021.
- [4] P. C. Chen, V. Malbasa, Y. Dong, and M. Kezunovic, "Sensitivity analysis of voltage sag-based fault location with distributed generation," IEEE Transactions on Smart Grid, vol. 6, no. 4, pp. 2098–2106, 2015.
- [5] M. Kashyap, A. Mittal, and S. Kansal, "Optimal placement of distributed generation using genetic algorithm approach," Lecture Notes in Electrical Engineering, vol. 476, pp. 587–597, 2019.
- [6] S. R. Ramavat, S. P. Jaiswal, N. Goel, and V. Shrivastava, "Optimal location and sizing of DG in the distribution system and its cost-benefit analysis," Advances in Intelligent Systems and Computing, vol. 698, pp. 103–112, 2019.
- [7] T. S Tawfeek, A. H. Ahmed, and S. Hasan, "Analytical and particle swarm optimization algorithms for optimal allocation of four different distributed generation types in radial distribution networks," Energy Procedia, vol. 153, pp. 86–94, 2018.
- [8] S. Mirsaeidi, S. Li, S. Devkota et al., "Reinforcement of power system performance through optimal allotment of distributed generators using metaheuristic optimization algorithms," Journal of Electrical Engineering & Technology, vol. 17, no. 5, pp. 2617–2630, 2022.
- [9] Adeagbo, A.; Olaniyi, E.; Ofoegbu, E.; Abolarin, A. Solar photo-voltaic system efficiency improvement using unitary-axis active tracking system. Int. J. Sci. Eng. Res. 2020, 11, 502–508.
- [10] Adewuyi, O.B.; Ahmadi, M.; Olaniyi, I.O.; Senjyu, T.; Olowu, T.O.; Mandal, P. Voltage security-constrained optimal generation rescheduling for available transfer capacity enhancement in deregulated electricity markets. Energies 2019, 12, 4371.
- [11] Hemeida MG, Ibrahim AA, Mohamed AA, et al. Optimal allocation of distributed generators DG

- based Manta Ray Foraging Optimization algorithm (MRFO). Ain Shams Eng J, 2021, 12:609–619.
- [12] Shradha SinghPariharNitinMalik, Analysing the impact of optimally allocated solar PV-based DG in harmonics polluted distribution network, Sustainable Energy Technologies and Assessments Volume 49, February 2022.
- [13] Abou El-Ela AA, El-Sehiemy RA, Abbas AS. Optimal placement and sizing of distributed generation and capacitor banks in distribution systems using water cycle algorithm. IEEE Syst J, 2018, 12:3629-3636.
- [14] Varaprasad Janamala, K Radha Rani, Optimal allocation of solar photovoltaic distributed generation in electrical distribution networks using Archimedes optimization algorithm Clean Energy, Volume 6, Issue 2, April 2022, Pages 271–287.
- [15] G. Guerra, J. a Martinez, and S. Member, "A Monte Carlo Method for Optimum Placement of Photovoltaic Generation Using a Multicore Computing Environment," PES Gen. Meet. Conf. Expo. 2014 IEEE. IEEE, pp. 1–5, 2014.

- [16] Fahimeh Sayadi, Saeid Esmaeili, Farshid Keynia, Two-layer volt/var/total harmonic distortion control in distribution network based on PVs output and load forecast errors, IET Generation, Transmission & Distribution, Volume 11,2016.
- [17] Fahimeh Sayadi, Saeid Esmaeili, Farshid Keynia, Feeder reconfiguration and capacitor allocation in the presence of non-linear loads using new P-PSO algorithm, IET Generation, Transmission & Distribution, Volume 10, 2015.
- [18] Calderaro V, Conio G, Galdi V, Massa G, Piccolo A. Optimal decentralized voltage control for distribution systems with inverter-based distributed generators. IEEE Trans Power Syst 2014; 29:230–41.
- [19] Van den Bergh, F., Engelbrecht, A., A Cooperative approach to particle swarm optimization. IEEE Transactions on Evolutionary Computation: 225-239, 2004.